Shape Coexistence at Zero Spin in ^{64}Ni driven by the Monopole Tensor Interaction

N. Mărginean[*,1] D. Little,[2,3] Y. Tsunoda,[4] S. Leoni[†,5,6] R. V. F. Janssens[‡,2,3] B. Fornal[§,7] T. Otsuka,[8,9,10] C. Michelagnoli,[11] L. Stan,[1] F. C. L. Crespi,[5,6] C. Costache,[1] R. Lica,[1] M. Sferrazza,[12] A. Turturica,[1] A. D. Ayangeakaa,[13] K. Auranen[¶,14] M. Barani,[5,6,11] P. C. Bender,[15] S. Bottoni,[5,6] M. Boromiza,[1] A. Bracco,[5,6] S. Călinescu,[1] C. M. Campbell,[16] M. P. Carpenter,[14] P. Chowdhury,[15] M. Ciemała,[7] N. Cieplicka-Oryǹczak,[7] D. Cline,[17] C. Clisu,[1] H. L. Crawford,[16] I. E. Dinescu,[1] D. Filipescu,[1] N. Florea,[1] A. M. Forney,[18] S. Fracassetti[**,5,6] A. Gade,[19,20] I. Gheorghe,[1] A. B. Hayes,[21] I. Harca,[1] J. Henderson,[22] A. Ionescu,[1] Ł. W. Iskra,[6] M. Jentschel,[11] F. Kandzia,[11] Y. H. Kim,[11] F. G. Kondev,[14] G. Korschinek,[23] U. Köster,[11] Krishichayan,[3] M. Krzysiek,[7] T. Lauritsen,[14] J. Li[††,14] R. Mărginean,[1] E. A. Maugeri,[24] C. Mihai,[1] R. E. Mihai,[1] A. Mitu,[1] P. Mutti,[11] A. Negret,[1] C. R. Niţă,[1] A. Olăcel,[1] A. Oprea,[1] S. Pascu,[1] C. Petrone,[1] C. Porzio,[5,6] D. Rhodes,[19,20] D. Seweryniak,[14] D. Schumann,[24] C. Sotty,[1] S. M. Stolze,[14] R. Şuvăilă,[1] S. Toma,[1] S. Ujeniuc,[1] W. B. Walters,[18] C. Y. Wu,[22] J. Wu,[14] S. Zhu,[21] and S. Ziliani[5,6]

[1]Horia Hulubei National Institute of Physics and Nuclear Engineering - IFIN HH, Bucharest, 077125, Romania
[2]Dept. of Physics and Astronomy, University of North Carolina at Chapel Hill, Chapel Hill, North Carolina 27599-3255, USA
[3]Triangle Universities Nuclear Laboratory, Duke University, Durham, North Carolina 27708-2308, USA
[4]Center for Nuclear Study, The University of Tokyo, 7-3-1 Hongo, Bunkyo, Tokyo 113-0033, Japan
[5]Dipartimento di Fisica, Università degli Studi di Milano, I-20133 Milano, Italy
[6]INFN sezione di Milano via Celoria 16, 20133, Milano, Italy
[7]Institute of Nuclear Physics, PAN, 31-342 Kraków, Poland
[8]Department of Physics, The University of Tokyo, 7-3-1 Hongo, Bunkyo, Tokyo 113-0033, Japan
[9]RIKEN Nishina Center, 2-1 Hirosawa, Wako, Saitama 351-0198, Japan
[10]KU Leuven, Instituut voor Kern- en Stralingsfysica, 3000 Leuven, Belgium
[11]Institut Laue-Langevin (ILL), 71 Avenue des Martyrs, 38042 Grenoble, France
[12]Département de Physique, Université libre de Bruxelles, B-1050 Bruxelles, Belgium
[13]Department of Physics, United States Naval Academy, Annapolis, Maryland 21402, USA
[14]Physics Division, Argonne National Laboratory, Argonne, Illinois 60439, USA
[15]Department of Physics and Applied Physics, University of Massachusetts Lowell, Lowell, Massachusetts 01854, USA
[16]Nuclear Science Division, Lawrence Berkeley National Laboratory, Berkeley, California 94720, USA
[17]Department of Physics and Astronomy, University of Rochester, Rochester, New York 14627, USA
[18]Department of Chemistry and Biochemistry, University of Maryland, College Park, Maryland 20742, USA
[19]Department of Physics and Astronomy, Michigan State University, East Lansing, Michigan 48824, USA
[20]National Superconducting Cyclotron Laboratory,
Michigan State University, East Lansing, Michigan 48824, USA
[21]National Nuclear Data Center, Brookhaven National Laboratory, Upton, New York 11973-5000, USA
[22]Lawrence Livermore National Laboratory, Livermore, California 94550, USA
[23]Technische Universitat Munchen, Munchen, Germany
[24]Paul Scherrer Institut, Villigen, Switzerland
(Dated: June 24, 2020)

The low-spin structure of the semi-magic ^{64}Ni nucleus has been considerably expanded: combining four experiments, several 0^+ and 2^+ excited states were identified below 4.5 MeV, and their properties established. The Monte Carlo shell model accounts for the results and unveils an unexpectedly-complex landscape of coexisting shapes: a prolate 0^+ excitation is located at a surprisingly high energy (3463 keV), with a collective 2^+ state 286 keV above it, the first such observation in Ni isotopes. The evolution in excitation energy of the prolate minimum across the neutron $N = 40$ sub-shell gap highlights the impact of the monopole interaction and its variation in strength with N.

In mesoscopic systems with many degrees of freedom (e.g., molecules, atomic nuclei, etc.), deformation is a common phenomenon resulting from symmetry breaking associated with quantum-mechanical states (practically)

————

[*]Corresponding authors: Nicu@tandem.nipne.ro
[†]Corresponding authors: Silvia.Leoni@mi.infn.it
[‡]Corresponding authors: Rvfj@email.unc.edu
[§]Corresponding authors: Bogdan.Fornal@ifj.edu.pl
[¶]Present address: Department of Physics, University of Jyvaskyla, P.O. Box 35, 40014, Jyvaskyla, Finland
[**]Present address: KU Leuven, Instituut voor Kern- en Stralingsfysica, 3000 Leuven, Belgium

————

[††]Present address: Department of Physics and Astronomy and National Superconducting Cyclotron Laboratory, Michigan State University, East Lansing, Michigan 48824, USA

degenerate in energy. The concept was originally introduced by Jahn and Teller who demonstrated that, in non-linear molecules, coupling between degenerate electronic states and collective vibrations can destroy the system's original symmetry [1]. In atomic nuclei, the appearance of ellipsoidal deformation can be viewed as a realization of this effect with specific superpositions of spherical single-particle states (e.g., Nilsson model [2]) induced by deformed mean potentials (mean-field approaches) [3, 4], or by quadrupole correlations (shell-model descriptions) [5, 6], highlighting the interplay between single-particle states and collective modes.

Among the features associated with deformation figures shape coexistence: a phenomenon ubiquitous throughout the nuclear chart [7, 8] where different shapes are present at comparable excitation energies. A clear-cut signature for its occurrence in even-even systems is the presence of low-lying 0^+ excitations residing in local minima of the nuclear potential energy surface (PES) in deformation space.

Over the past two decades, studies of neutron-rich nuclei have highlighted the contribution of the monopole component of the tensor force to the evolution of the structure of exotic nuclei [6, 9], especially in the change in single-particle (or shell) structure with neutron excess, with some magic numbers vanishing and other, new ones appearing [10]. Besides such single-particle properties, its role in driving the nuclear shape was subsequently identified [6, 11–15], specifically in connection with shape coexistence.

Neutron-rich even $_{28}$Ni isotopes are a noteworthy example of shape coexistence: ^{68}Ni was shown to exhibit a spherical ground state, while the 1605-keV, 0_2^+ and 2511-keV, 0_3^+ levels are understood as oblate and prolate excitations [11, 16–21]. In ^{70}Ni, a prolate 0_2^+ state was found 1567 keV above the spherical ground state [22]. Finally, four 0^+ levels are known below a 4 MeV excitation energy in ^{66}Ni, where the ground state and the 2664-keV 0_3^+ level are interpreted as spherical, while the 0_2^+, 2445-keV and the 0_4^+, 2945-keV states are of oblate and prolate character [23].

The present paper focuses on ^{64}Ni, the heaviest, stable nucleus in the isotopic chain, and reveals a complex landscape in deformation that was not anticipated by mean-field calculations [24–28], which predicted a single, spherical minimum in the PES, the development of a secondary prolate minimum occurring only in heavier isotopes. In contrast, recent MCSM calculations [11], performed in a large model space, indicate coexistence of spherical and deformed oblate and prolate 0^+ states already in ^{62,64}Ni, and their observation would demonstrate the impact of the monopole tensor force already at the valley of stability. This Letter reports extensive tests of these MCSM predictions. Besides the customary data on level energies, spins and parities, comparisons also extend to state lifetimes, transition probabilities, branching and multipole mixing ratios. To achieve the required sensitivity and provide as complete information on 0^+ states as possible, four experiments; i.e., transfer reactions, neutron capture, Coulomb excitation and nuclear resonance fluorescence had to be carried out at the IFIN-HH Tandem Laboratory (Bucharest, Romania), the Institut Laue-Langevin (ILL, Grenoble, France), the Argonne National Laboratory (ANL, Argonne, USA) and the Triangle Universities Nuclear Laboratory (TUNL, Duke Univ., USA), respectively. Results from the first three techniques are reported below [46].

Prior to this work, two excited 0^+ states had been identified in ^{64}Ni, at 2867 and 3026 keV, following β-decay and (t,p)-reaction studies [29, 30]. These levels were subsequently confirmed in deep-inelastic reaction measurements [31], and their γ decay to the 1346-keV 2_1^+ state was observed. Candidates for other, higher-lying 0^+ levels were also reported from the (t,p) and β-decay data, and from double-neutron capture [32].

At IFIN-HH, ^{64}Ni was populated by ^{62}Ni(^{18}O,^{16}O) two-neutron (2n) transfer on a 5 mg/cm^2-thick target, with a 39-MeV beam energy; i.e., just below the Coulomb barrier in order to reduce competition from fusion-evaporation. Transitions of interest were measured with ROSPHERE, an array of 25 Compton-suppressed HPGe detectors with $\sim$2% total efficiency at 1.3 MeV [33]. The same reaction, but with a thinner, 0.92 mg/cm^2 target and a 5 mg/cm^2-Ta stopper, placed at six distances from the target (10, 17, 25, 45, 100 and 150 μm), was employed for lifetime measurements via the recoil-distance technique. The sub-barrier transfer reaction ^{65}Cu(^{11}B,^{12}C)^{64}Ni at 26 MeV on a 7.22 mg/cm^2-thick target was performed as well [34].

The coincidence spectrum, from the thick target 2n-transfer reaction, gated on the 1346-keV $2_1^+ \rightarrow 0_1^+$ ^{64}Ni transition, is presented in Fig. 1. All visible lines correspond to ^{64}Ni transitions which deexcite states below 4.6 MeV, with spin up to 7^- [31]. The 1521- and 1680-keV γ rays, depopulating the known 0_2^+ and 0_3^+ states, are clearly visible. Their respective half-lives, as measured in the plunger experiment, are $T_{1/2}$=1.4(6) and 3.6(1.2) ps (inset of Fig. 1) [34]. A search for transitions from higher-lying candidate 0^+ states proved inconclusive in the IFIN-HH data sets.

A twenty-day experiment was then conducted at ILL [35], where ^{64}Ni was populated via thermal-neutron capture on a 2 GBq ^{63}Ni sample (extracted from a larger CERN-nTOF sample [36]), where 12.1 mg of NiO grains were glued between two 6 μm-thick Al foils and contained $\approx$ 8% ^{63}Ni ($T_{1/2}$ = 101.2(15) y), 69% ^{62}Ni, <3% ^{63}Cu and other Ni isotopes, and 20% O. The spectra were dominated by transitions in ^{63}Ni and ^{64}Ni. The γ rays were detected with FIPPS [37], a $\sim$3.7% efficient array of 16 clover detectors (8 on loan from IFIN-HH) arranged in a 4π geometry, particularly suitable for angular correlation studies in view of the large number (71) of relative angles
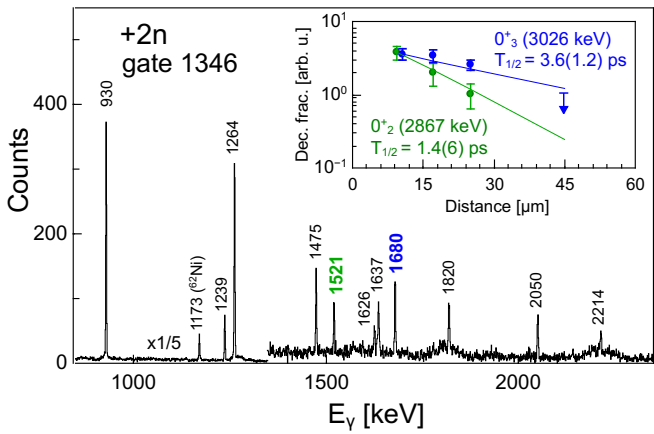
FIG. 1: 2n-transfer reaction: partial spectrum in coincidence with the ^{64}Ni $2_1^+ \rightarrow 0_1^+$ transition (thick-target data). Inset: decay curves from the plunger experiment for the 1521- and 1680-keV transitions linking the 0_2^+ and 0_3^+ levels to the 2_1^+ state.

between the germanium crystals.

The $1/2^-$ spin-parity of the ^{63}Ni ground state results in a 0^- or 1^- ^{64}Ni capture state at 9657.47 keV, and strong population of 0^+, 1^+ and 2^+ levels through $E1$ primary γ rays is expected. Direct feeding of the known 0_2^+ and 0_3^+ states, at 2866.9 and 3025.5 keV, is clearly visible in coincidence spectra gated on respective 6791- and 6632-keV primary transitions. Figure 2(a) displays the 6632-keV gated spectrum where both the $0_3^+ \rightarrow 2_1^+$, 1680-keV transition and a new, weaker (3.6(2)% of the former) 749-keV, $0_3^+ \rightarrow 2_2^+$ decay branch are observed. The angular correlation for the $0_3^+ \rightarrow 2_1^+ \rightarrow 0_1^+$ cascade (inset, Fig. 2(a)) agrees with the 0^+ spin-parity assignment to the 3026-keV level. A search for additional 0^+ excited states was undertaken by considering every primary transition in coincidence with the 1346-keV ground-state transition, and also feeding levels in the 3-6 MeV excitation energy range. Five such high-energy transitions, at 6194, 5801, 5389, 4954 and 3889 keV, populating states at 3463.1, 3856.0, 4268.1, 4703.9 and 5768.6 keV were found to exhibit decay patterns consistent with 0^+ spin-parity assignments. Further, the angular correlation analysis yielded firm 0^+ assignments for the states at 3463.1, 4268.1, 4703.9 and 5768.6 keV, by considering in each case pairs of γ rays composed, on the one hand, of the decay branch to the 2_1^+ state and, on the other, of the $2_1^+ \rightarrow 0_1^+$, 1346-keV transition. The relevant analysis for the 0_4^+, 3463.1-keV level is illustrated in Fig. 2(b) [47].

The partial level scheme is given on the left of Fig. 3. The 0_4^+ state at 3463 keV is of particular interest; it was observed earlier with tentative $(2^{+/-}, 3^-)$ [31] and $(0^+, 1, 2, 3^-)$ spin-parity assignments [32], but is firmly assigned here. It should be emphasized that this level is not populated in ^{64}Co β-decay [29], in contrast to all

other 0^+ states, up to 0_6^+, which are fed in this process. This observation already points to a marked difference in structure for this excitation, and is reminiscent of that occurring in ^{66}Ni [23], where the prolate-deformed 0_4^+ state at 2974 keV was also the only 0^+ excitation not fed in the β-decay of the spherical ^{66}Co ground state [38]. Further inspection of the ILL data revealed three 2^+ states (firmly established in this work) at 3647.9, 3749.1 and 3798.7 keV, which complement four such excitations, at 1345.8, 2276.6, 2972.1 and 3276.0 keV, reported in Refs. [39] (see Fig. 3). The angular correlations for the transitions deexciting 2_4^+, 2_5^+ and 2_7^+ levels toward the 2_1^+ state all indicate a dominant $M1$ character, with only a small $E2$ admixture. This is illustrated through the representative data for the $2_5^+ \rightarrow 2_1^+ \rightarrow 0_1^+$ cascade of Fig. 2(c). A notable exception to this trend is the $2_6^+ \rightarrow 2_1^+ \rightarrow 0_1^+$ sequence where the 2403-keV γ ray exhibits a pronounced $E2$ character, as strikingly illustrated by comparing Figs. 2(c) and (d). The corresponding mixing ratio was determined to be $\delta = +1.23(10)$. Furthermore, from the line shape observed for this 2403-keV γ ray in spectra following proton transfer, a lower limit of 0.5 ps was obtained for the 2_6^+ state half-life, which results in upper limits to the respective $B(E2)$ strengths of 0.02, 0.4, and 0.02 W.u. for the $2_6^+ \rightarrow 0_1^+$, $2_6^+ \rightarrow 2_1^+$ and $2_6^+ \rightarrow 2_2^+$ transitions. These all indicate that deexcitation from the 2_6^+ state is significantly hindered.

To gain further insight into the nature of the 0^+ and 2^+ excitations in ^{64}Ni, a multi-step Coulomb excitation (CE) measurement was carried out at the ATLAS facility at ANL. A 0.5 mg/cm^2 isotopically-enriched ^{208}Pb target was bombarded by a ^{64}Ni beam at an energy of 272 MeV, a value 14% below the Coulomb barrier. Transitions were detected with the GRETINA tracking array [40] in coincidence with the two reaction partners measured by the CHICO2 compact heavy ion counter [41], as described in Ref. [42]. The resulting yields were analyzed with the semi-classical Coulomb excitation code, GOSIA [43], which provided electromagnetic matrix elements for transitions from 13 states [44]. For the present paper, the following reduced transition probabilities are relevant: $B(E2; 2_1^+ \rightarrow 0_1^+) = 140(20)$ e^2fm^4, $B(E2; 2_2^+ \rightarrow 2_1^+) = 73(8)$ e^2fm^4, $B(E2; 0_2^+ \rightarrow 2_1^+) = 48(3)$ e^2fm^4, $B(E2; 0_3^+ \rightarrow 2_1^+) = 10(1)$ e^2fm^4, $B(E2; 0_4^+ \rightarrow 2_1^+) < 1.3$ e^2fm^4 and $B(E2; 2_6^+ \rightarrow 2_2^+) < 3.2$ e^2fm^4. In terms of single-particle estimates, these values translate into strengths of 9(1), 4.8(5), 3.2(2), 0.65(7), <0.08 and <0.2 W.u., respectively. Good agreement is noted with the lifetime data for the 0_2^+ and 0_3^+ decays to the 2_1^+ state with $B(E2)$ values of 3.3(14) and 0.8(3) W.u., respectively (Fig. 1). The limits for the 2_6^+ and 0_4^+ states are also consistent, but somewhat tighter in the CE case.

The left part of Fig. 3 provides a ^{64}Ni level scheme encompassing states of positive parity with spins 0, 1, 2, up to 4.26 MeV excitation energy. The information gathered on mixing, branching ratios and transition strengths
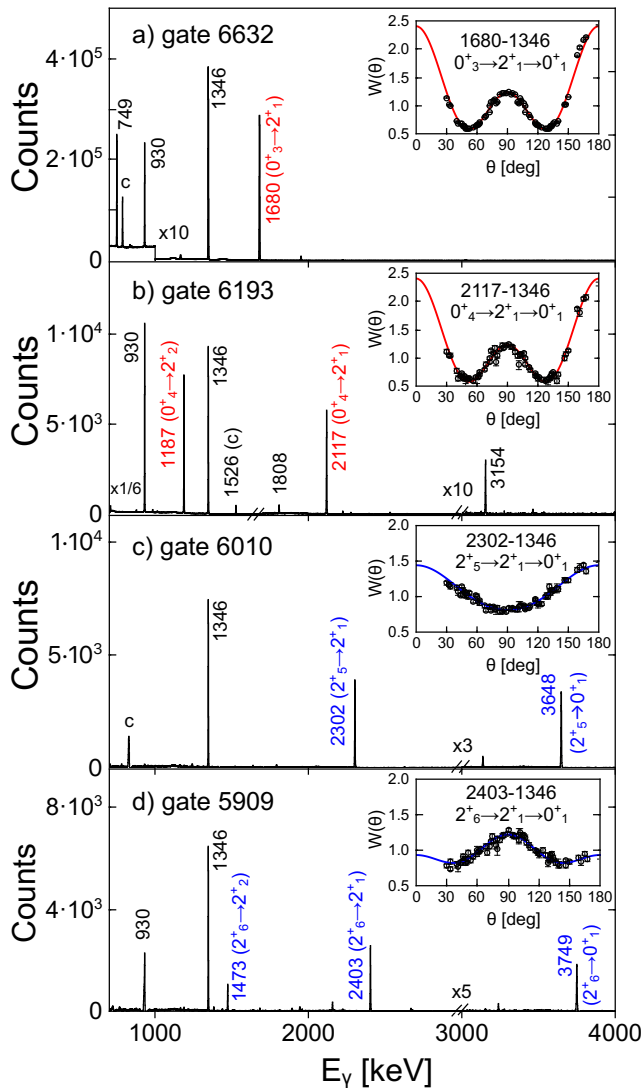
FIG. 2: Neutron-capture data: γ-ray spectra in coincidence with primary transitions (energy indicated in each panel). Relevant transitions are also labeled. Insets: measured angular correlations for the cascades indicated.

has been added to enable extensive comparisons with calculations. Such additional tests of theory are generally difficult, if not impossible, especially for neutron-rich nuclei requiring experiments with radioactive beams.

The right side of Fig. 3 presents the level scheme from MCSM calculations, performed with significantly extended MCSM basis vectors as compared to earlier studies of $^{66-78}$Ni [11, 23]. The model space includes protons and neutrons in the full fp shell with, in addition, the $g_{9/2}$ and $d_{5/2}$ orbitals, and the Hamiltonian is based on the A3DA-m effective interaction [11]. The transition probabilities were obtained with the usual effective charges ($e_p = 1.5\ e$, $e_n = 0.5\ e$), a spin quenching factor of 0.7 and an isovector orbital g-factor of 0.1. State energies are reproduced satisfactorily − the rms deviation

is $\sim$300 keV, commensurate with expectations for shell-model calculations. For the first three 0^+ excitations, the computed decay patterns mirror the data: the decay to the 2_1^+ level dominates the deexcitation from 0_2^+ and 0_3^+ states, and the intensity variation between the four 0_4^+ branches is qualitatively reproduced, with the $0_4^+ \rightarrow 2_2^+$ one being strongest. The change in $B(E2)$ strengths calculated for the $0_{2,3,4}^+ \rightarrow 2_1^+$ decays (i.e., 12, 2.4 and 5 10^{-4} W.u.) reproduces the data, even though the absolute strengths are larger. Finally, the MCSM calculations also reproduce the lack of feeding of the 0_4^+ state in β decay, when compared to that of the other 0^+ levels.

A sequence of relatively close-lying 2^+ levels is also predicted with deexcitation patterns and transition probabilities agreeing with observations, at least when the calculated 2_7^+ state is associated with the 2_6^+ experimental one − the 2_6^+ and 2_7^+ levels are computed to lie only 235 keV apart; i.e., within the expected accuracy of the A3DA-m interaction. Theory also reproduces (i) relative variations in $B(E2)$ values between the 2^+ levels (including the retardation for the transitions out of the 2_6^+ state, which agrees with the observed small $B(E2)$ upper limits), and (ii) the strong $E2$ component in the $\Delta I = 1$, $2_6^+ \rightarrow 2_1^+$ transition, where the measured mixing ratio $\delta(E2/M1) = +1.23(10)$ (vs. $\delta_{\text{MCSM}}=2.6$) contrasts those for similar transitions from the other 2^+ excitations (Fig. 2 (c)).

According to the MCSM calculations, the first four 0^+ states are associated with spherical, oblate, spherical and prolate shapes, respectively. Thus, the $0_4^+ \rightarrow 2_1^+$ decay is a prolate-to-spherical shape-changing transition, resulting in significant retardation, in line with the $B(E2)$ limit of <0.08 W.u. The same picture applies to the computed 2_7^+ level, which theory also locates in the prolate minimum. The observed decay pattern, the limits on the decay strengths and the dominant $E2$ character of the $2_6^+ \rightarrow 2_1^+$ transition argue in favor of this interpretation for the observed 2_6^+ state. Hence, based on the consistency between data and theory, this 2_6^+ level represents the first observation in the Ni isotopes of a 2^+ excited state in a well-isolated prolate potential minimum. The "shape-isomer"-like properties of the 0_4^+ excitation in ^{64}Ni mirror closely those found in ^{66}Ni [23] with, in addition, the observation of the first element of a rotational sequence. Using the Raman systematics, linking 2^+ energies to transition strengths [45], this results in a computed β_2 deformation of $\sim$0.4, in agreement with the MCSM result (Fig. 4(a)). The low-energy 286-keV in-band $2_6^+ \rightarrow 0_4^+$ transition, even with a calculated $B(E2)$ strength of $\sim$40 W.u., cannot be observed: the flux proceeds through high-energy (>1 MeV) $E2$ γ-rays due to the E_γ^5 factor.

With these new, extensive data in ^{64}Ni, the evolution in energy of the prolate minimum with N can now be traced in the Ni isotopes, revealing a sharp contrast with that exhibited by the 2_1^+ levels of spherical nature. The

FIG. 3: Comparison between data (left) and MCSM calculations (right) for ^{64}Ni level properties derived in this work. Quoted transition strengths are from CE, branchings and mixing ratios from neutron capture. Decays from prolate structures are highlighted in red.

latter are all in the 1250 - 1450 keV range, with the exception of the 2033-keV value for ^{68}Ni due to the $N = 40$ sub-shell closure. In contrast, the prolate 0^+ excitation rises from 1567 keV in ^{70}Ni, to 2511 and 2905 keV in ^{68}Ni and ^{66}Ni, and 3463 keV in ^{64}Ni. This behavior for $N < 40$ differs markedly from the lowering of deformed intruder states when moving away from a (sub)-shell closure, as observed in the Hg and Pb nuclei [7, 8], for example. Low-lying prolate intruder states in the aforementioned neutron-rich Ni isotopes reflect the action of the monopole tensor force which is often referred to as Type II shell evolution [12, 13, 23], and involves particle-hole excitations of neutrons to the $g_{9/2}$ unique-parity orbital from the fp shell. Extra binding for such intruder states is provided largely by the monopole tensor part of the nucleon-nucleon force (the proton $f_{5/2}$ - $f_{7/2}$ spin-orbit splitting is reduced, favoring proton excitations across the $Z = 28$ shell gap), which stabilizes isolated, deformed local minima in the PES (Fig. 4(a)). This additional binding is reduced for lower N values as there are progressively fewer neutrons which can be excited to the $g_{9/2}$ orbital. The deformed minimum rises in excitation energy as a result. As demonstrated in Fig. 4(b), by deactivating components of the monopole interaction (i.e., monopole frozen [6]), a nearly vanishing prolate minimum would reside at even higher excitation, in line with mean field predictions [24–28].

The present work has unveiled an unexpectedly complex landscape of nuclear deformation at zero spin in stable, semi-magic ^{64}Ni. This includes the first identification, in Ni isotopes, of a 2^+ excitation in the prolate minimum. The new results provide, for the first time, a complete picture of the mechanisms underlying the appearance of deformation and shape coexistence in the Ni isotopes. They highlight the impact of the monopole tensor interaction in driving deformation at zero spin, even in ^{64}Ni, a nucleus within the valley of stability.

FIG. 4: ^{64}Ni potential energy surfaces with (a) full, original interaction used in MCSM calculations, and (b) monopole-frozen interaction (i.e., the monopole component is subtracted from the proton-neutron interaction, and single-particle energies are adjusted to original effective values of the spherical minimum [6]).

[1] H. A. Jahn and E. Teller, Proc. Roy. Soc. A161, 220 (1937).
[2] A. Bohr, B. R. Mottelson, Nuclear Structure, I and II, W.A. Benjamin, 1975.
[3] P. -G. Reinhard and E. W. Otten, Nucl. Phys. A420, 173 (1984).
[4] W. Nazarewicz, Nuc. Phys. AA574, 27c (1994).
[5] Y. Utsuno, T. Otsuka, B. A. Brown, M. Honma, T. Mizusaki, N. Shimizu et al., Phys. Rev. C 86, 051301(R) (2012).
[6] T. Otsuka, Y. Tsunoda, T. Abe , N. Shimizu, P. Van Duppen, Phys. Rev. Lett. 123, 222502 (2019)
[7] J. L. Wood et al., Phys. Rep. 215, 101 (1992).
[8] K. Heyde and J. L. Wood, Rev. Mod. Phys. 83, 1467 (2011).
[9] T. Otsuka, T. Suzuki, M. Honma, Y. Utsuno, N. Tsunoda, K. Tsukiyama, M. Hjorth-Jensen, Phys. Rev. Lett. 104, 012501 (2010).
[10] T. Otsuka, A. Gade, O. Sorlin, T. Suzuki, and Y. Utsuno, Rev. Mod. Phys. 92, 015002 (2020).
[11] Y. Tsunoda, T. Otsuka, N. Shimizu, M. Honma, Y. Utsuno, Phys. Rev. C 89, 031301(R) (2014).
[12] T. Otsuka and Y. Tsunoda, J. Phys. G: Nucl. Part. Phys. 43 024009 (2016)
[13] T. Togashi, Y. Tsunoda, T. Otsuka, and N. Shimizu, Phys. Rev. Lett. 117, 172502 (2016).
[14] B. A. Marsh et al., Nat. Phys. 14, 1163 (2018).
[15] S. Sels, T. DayGoodacre, B. A. Marsh, A. Pastore, W. Ryssens, Y. Tsunoda, et al., Phys. Rev. C 99, 044306 (2019).
[16] B. P. Crider et al., Phys. Lett. B763, 108 (2016).
[17] S. Suchyta, S. N. Liddick, Y. Tsunoda, T. Otsuka, M. B. Bennett, A. Chemey et al., Phys. Rev. C 89, 021301(R) (2014).
[18] F. Recchia, C. J. Chiara, R. V. F. Janssens, D. Weisshaar, A. Gade, W. B. Walters et al., Phys. Rev. C 88, 041302(R) (2013).
[19] F. Flavigny, D. Pauwels, D. Radulov, I. J. Darby, H. DeWitte, J. Diriken et al., Phys. Rev. C 91, 034310 (2015).
[20] W. F. Mueller, B. Bruyneel, S. Franchoo, M. Huyse, J. Kurpeta, K. Kruglov et al., Phys. Rev. C 61, 054308 (2000).
[21] C. J. Chiara, R. Broda, W. B. Walters, R. V. F. Janssens, M. Albers, M. Alcorta et al., Phys. Rev. C 86, 041304(R)(2012).
[22] C. J. Prokop, B. P. Crider, S. N. Liddick, A. D. Ayangeakaa, M. P. Carpenter, J. J. Carroll et al., Phys. Rev. C 92, 061302(R) (2015).
[23] S. Leoni, B. Fornal, N. Marginean, M. Sferrazza, Y. Tsunoda, T. Otsuka et al., Phys. Rev. Lett. 118, 162502 (2017).
[24] S. Hilaire and M. Girod, Eur. Phys. J. A33, 237 (2007).
[25] J. F. Berger, M. Girod and D. Gogny, Comp. Phys. Comm. 63, 365 (1991).
[26] J. Decharge and D. Gogny, Phys. Rev. C 21, 1568 (1980).
[27] P. Möller, A. J. Sierk, and A. Iwamoto, Phys. Rev. Lett. 92, 072501 (2004).
[28] P. Möller, A. J. Sierk, R. Bengtsson, H. Sagawa, and T. Ichikawa, Phys. Rev. Lett. 103, 212501 (2009).
[29] D. Pauwels, D. Radulov, W. B. Walters, I. G. Darby,H. DeWitte, J. Diriken et al., Phys. Rev. C 86, 064318(2012).
[30] W. Darcey, R. Chapman, and S. Hinds, Nucl. Phys. A170, 253 (1971).
[31] R. Broda, T. Pawlat, W. Krolas, R. V. F. Janssens, S. Zhu, W. B. Walters et al., Phys. Rev. C 86, 064312 (2012).
[32] A. Harder et al., Z. Phys. A 343, 7 (1992).
[33] D. Bucurescu et al., Nucl. Instrum. Methods Phys. Res., Sect. A 837, 1 (2016).
[34] L. Stan et al., to be published.
[35] N. Mărginean et al., to be published.
[36] C. Lederer et al., Phys. Rev. C 89, 025810 (2014).
[37] C. Michelagnoli et al., EPJ 193, 04009 (2018).
[38] M. Stryjczyk, Y. Tsunoda, I. G. Darby, H. DeWitte, J. Diriken, D. V. Fedorov et al., Phys. Rev. C 98, 064326 (2018).
[39] Nuclear Data Center, Brookhaven National Laboratory, https://www.nndc.bnl.gov.
[40] S. Paschalis, I. Y. Lee, A. O. Macchiavelli, C. M. Campbell, M. Cromaz, S. Gros, J. Pavan, J. Qian, R. M. Clark, H. L. Crawford, D. Doering, P. Fallon, C. Lionberger, T. Loew, M. Petri, T. Stezelberger, S. Zimmermann, D. C. Radford, K. Lagergren, D. Weisshaar, R. Winkler, T. Glasmacher, J. T. Anderson, C. W. Beausang, Nucl. Instrum. Methods Phys. Res. A 709, 44 (2013).
[41] C. Y. Wu, D. Cline, A. Hayes, R. S. Flight, A. M. Melchionna, C. Zhou, I. Y. Lee, D. Swan, R. Fox, J.T. Anderson, Nucl. Instrum. Methods Phys. Res. A 814, 6 (2016).
[42] A. D. Ayangeakaa, R. V. F. Janssens, S. Zhu, D. Little, J. Henderson, C. Y. Wu, D. J. Hartley, M. Albers, K. Auranen, B. Bucher, M. P. Carpenter, P. Chowdhury, D. Cline, H. L. Crawford, P. Fallon, A. M. Forney, A. Gade, A. B. Hayes, F. G. Kondev, Krishichayan, T. Lauritsen, J. Li, A. O. Macchiavelli, D. Rhodes, D. Seweryniak, S. M. Stolze, W. B. Walters, and J. Wu, Phys. Rev. Lett. 123, 102501 (2019).
[43] T. Czosnyka, D. Cline, and C. Y. Wu, Bull. Am. Phys. Soc. 28, 745 (1983), and Gosia Manual," http://www.pas.rochester.edu/ cline/Gosia/ (2012).
[44] D. Little, R. V. F. Janssens, A. D. Ayangeakaa et al., to be published and D. Little, PhD dissertation, Univ. North Carolina at Chapel Hill, unpublished (2020).
[45] Atomic Data and Nuclear Data Tables 78, 1-128 (2001).
[46] The results from the nuclear resonance fluorescence ex-

periment confirm those discussed in the present letter, and will be published elsewhere (U. Friman-Gayer et al., to be published).

[47] For the 3856.0-keV level, the 0^+ assignment was established via the 702-3154 keV correlation cascade, involving the intermediate 1^+ state at 3154 keV, first identified in this work [35]).